PRACE INSTYTUTU ODLEWNICTWA
TRANSACTIONS OF FOUNDRY RESEARCH INSTITUTE

Volume LVII Year 2017 Number 4

High-temperature interaction of molten vermicular graphite cast iron with Al_2O_3 substrate

Magdalena Bacior[1], Natalia Sobczak[2,3], Marta Homa[2], Patrycja Turalska[2], Artur Kudyba[2], Grzegorz Bruzda[2], Rafał Nowak[2], Andrzej Pytel[2]

[1]University of Agriculture in Krakow, Department of Physics, al. A. Mickiewicza 21, 31-120 Krakow, Poland
[2]Foundry Research Institute, ul. Zakopiańska 73, 30-418 Krakow, Poland
[3]Institute of Precision Mechanics, ul. Duchnicka 3, 01-796 Warsaw, Poland

E-mail: m.bacior@ur.krakow.pl

Received: 06.11.2017. Accepted in revised form: 29.12.2017.

DOI: 10.7356/iod.2017.41

Abstract

The wetting behavior and reactivity between molten cast iron (originally vermicular graphite cast iron, containing in wt. %: 3.70 C, 2.30 Si, 0.44 Mn, 0.054 P, 0.017 Mg, 0.015 S) and commercial polycrystalline alumina (Al_2O_3 substrate of 99.70% purity and less than 3 vol. % porosity) were investigated. The wettability test was performed under an inert flowing gas atmosphere (Ar, 850−900 hPa) at a temperature of 1450°C for 15 min using a sessile drop method combined with classical contact heating procedure.

The high temperature interaction between molten cast iron sample and Al_2O_3 substrate was continuously recorded with a high-speed high-resolution CCD camera. The results showed that the molten cast iron does not wet the Al_2O_3 substrate (θ = 131°).

After wettability test, the cross-sectioned sessile drop couple was examined using scanning electron microscopy coupled with X-ray energy dispersive spectroscopy. It was found that in the solidified cast iron drop, the graphite phase took the shape of flakes having a different dispersion degree, i.e. vermicular precipitates of graphite did not re-grow during solidification of the drop. Moreover, structural characterization of the drop/substrate interface revealed the layer of about 26 μm thick composed mainly of carbon and located at the drop-side interface while at the substrate-side interface, the reaction zone (~70 μm) formed due interaction between Al_2O_3 and molten cast iron was well distinguished.

Keywords: *vermicular graphite cast iron, Al_2O_3, sessile drop method, wetting kinetics, reactivity*

1. Introduction

Vermicular graphite cast iron (VG iron) is an engineering material, which has recently become more and more popular [1−7] due to its favorable combination of mechanical, thermal properties and utility properties. Among others, the VG cast iron has higher values of tensile strength, elongation, field strength, fatigue strength, modulus of elasticity as well as resistance to oxidation at elevated temperatures, than flake graphite (FG) cast iron. VG cast iron is widely used for the production of brake discs in cars and trains, blocks of cylinder, heads, parts of agricultural machinery as well as many other components working at elevated temperatures. VG cast iron takes an intermediate place between FG cast iron and nodular graphite (ND) cast iron. Compared to ND cast iron, VG cast iron has higher damping capacity, higher thermal conductivity, better castability and lower tendency for contraction cavity formation [8−11].

Numerous studies have been carried out in recent years to understand the process of crystallization of different type of cast iron and factors affecting the morphology of graphite precipitates and the structure-properties relationships of solidified castings [12−15].

One of the factors that might influence the structure formation is the material of ceramic mould used in casting processing. Despite numerous investigations of VG cast iron undertaken in recent years, the research of high temperature phenomena occurring in molten alloy (originally with a VG cast iron structure) as well as its interaction with oxide-based refractories (used for mould production) have not been undertaken so far. Understanding the high-temperature processes occurring in the cast iron/oxide systems could help to explain the

phenomenon of cast iron oxidation, which takes place during the metallurgical process since metal oxides are commonly used as the linings of furnaces and vats in practice of cast iron production.

Moreover, the knowledge gained about high-temperature interaction between cast irons and metal oxides could be also used by specialists in the field of metallurgy and foundry to develop new oxide coatings for metal molds or for the production of high quality defect-free cast iron castings.

Finally, information on high-temperature behavior of molten cast irons in contact with various ceramics is of practical importance for the development of new generation metal matrix composites, i.e. cast iron matrix composites reinforced with ceramic phase [16,17] or ceramic inserts [18].

This work is focused on high-temperature interaction between VG cast iron with polycrystalline alumina, widely used in metal casting practice and which is a reference material for the subsequent investigations of the effect of alloying additions on thermophysical properties of molten cast iron as well as its wettability and reactivity in contact with metal oxides.

2. Materials and testing

2.1. Materials

The material for wettability test was hypereutectic vermicular graphite cast iron with a saturation coefficient S_c = 1.04, evaluated from Equation (1) [19]:

$$S_c = \frac{C}{4.26 - 0.30 \cdot Si - 0.36 \cdot P - 0.40 \cdot S + 0.027 \cdot Mn} \quad (1)$$

where C is a total carbon while *Si*, *P*, *Mn* mean the content of each elements in the sample of cast iron, expressed in weight percentages. Melting and casting trial of the cast iron with vermicular graphite were carried according with the procedure described elsewhere [20]. The chemical composition of selected VG cast iron at as-cast state is presented in Table 1. The sample of cast iron was cut from a large casting to get the sample with cubic shape of 5 × 5 × 5 mm dimensions.

Table 1. The chemical composition of vermicular graphite cast iron sample, wt. %

	C	Si	Mn	P	S	Mg
VG cast iron	3.70	2.30	0.44	0.054	0.015	0.017

For the wettability measurements, commercial polycrystalline alumina (Al_2O_3 substrate of 99.7% purity and open porosity below 3 vol. %) of a cylindrical shape (18 mm in diameter and 5 mm high), produced by Ceramit (Poland), was used. The surface roughness of the Al_2O_3 substrate was R_a = 152.5 nm.

2.2. Research procedure

Wettability test was performed by a sessile drop method using the experimental complex (Fig. 1) for high-temperature studies of liquid metals and alloys available at the Centre for High Temperature Studies of the Foundry Research Institute [21−25]. Directly before loading into vacuum chamber, the VG cast iron sample was mechanically and ultrasonically cleaned in isopropanol, placed on the Al_2O_3 substrate and located inside a tantalum resistant heater of vacuum chamber.

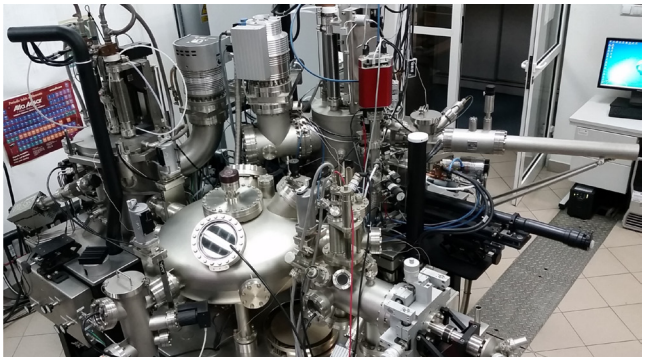

Fig. 1. Experimental complex for high-temperature studies of interaction between liquid metals and alloys with refractory materials [23]

After evacuation of gases and getting vacuum of p = 2 × 10^{-6} mbar by means of a turbomolecular pump, the couple of materials (VG cast iron sample on Al_2O_3 substrate) was contact heated with a rate of about 15°C/min up to 500°C. Then the argon (99.9992% purity) was introduced into a vacuum chamber and the couple was heated up, with the same rate to a test temperature of 1450°C. After 15 min of the high-temperature investigation at 1450°C (p = 870 mbar), the couple was cooled to room temperature with a rate of 20°C/min (Fig. 2).

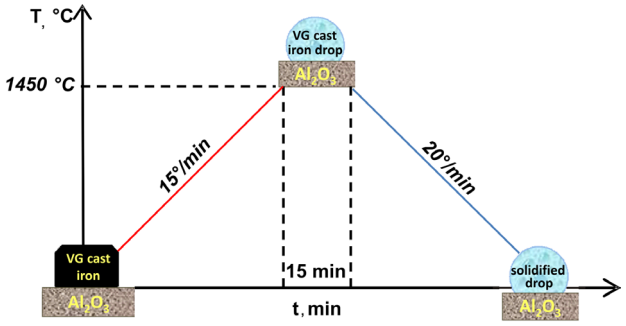

Fig. 2. Scheme illustrating the contact heating (CH) procedure of the sessile drop method used in wetting test with cast iron on Al_2O_3

The high temperature interaction in the cast iron/Al_2O_3 couple was recorded using high-speed high-resolution CCD camera MC1310 with a rate of 10 fps (frames per second) during melting of metal sample and during isothermal heating of the wetting test. During cooling to the solidification temperature, the recording was carried out at a rate of 1 fps.The collected images were used for estimation the contact angle values with a use of ASTRA2 software (CNR-IENI, Italy [26,27]) as well as for making a real-time movie of high-temperature test performed. The software enables the determination of the contact angle on the left (θ_l) and on the right (θ_r) sides of a drop by an automatic image analysis with systematic uncertainty of the contact angle less than ±2°.

The detailed structural investigation was performed on both the starting material (VG cast iron sample) and the solidified cross-section of the cast iron/Al_2O_3 couple by scanning electron microscopy (SEM) using TM3000 HITACHI device equipped with energy-dispersive X-ray spectroscopy (EDS) analyzer (Quantax 70) and using Zeiss Observer 21m optical microscope (OM).

3. Results and discussion

Figures 3a–i present the real observation of melting and solidification process of the selected VG cast iron sample on the alumina substrate. The beginning of the melting process of initially solid sample started at T = 1182°C (Fig. 3b), while the wetting kinetics was recorded from T = 1191°C (Fig. 3c), when the drop was formed. Further heating of the sample to the test temperature of 1450°C caused a change of the drop shape (Figs. 3c–d). During cooling of the couple up to T = 1119°C (Figs. 3f–i), a small secondary droplet (daughter drop) was created on the left side of the "mother" drop (Fig. 3g), and then at 1102°C, another droplet was created at the right side of the drop (Fig. 3h). The final image of the couple at the end of the experiment is presented in Figure 3i.

Figure 4 shows the evolution of contact angle (θ) as a function of time and temperature within the wettability test of the VG cast iron/Al_2O_3 couple.

In this test, of the contact angles were measured when the system reached T = 1191°C since at this temperature, the sample of VG cast iron began to melt. As shown in Figure 5, liquid cast iron did not wet (θ >90°) the alumina substrate forming the contact angle θ_l* = 149° and θ_r* = 147°. During further heating of the cast iron/Al_2O_3 couple to the test temperature, a decrease in the contact angle values was observed. At the beginning of the wettability test (T = 1450°C, t = 0), the values of the contact angles were: θ_l = 133° and θ_r = 129°, respectively. Holding the system at the test temperature within 15 minutes did not affect the value of the contact angle, whose average value, after 15 minutes of measurements at 1450°C, was θ_{fav} = 131°.

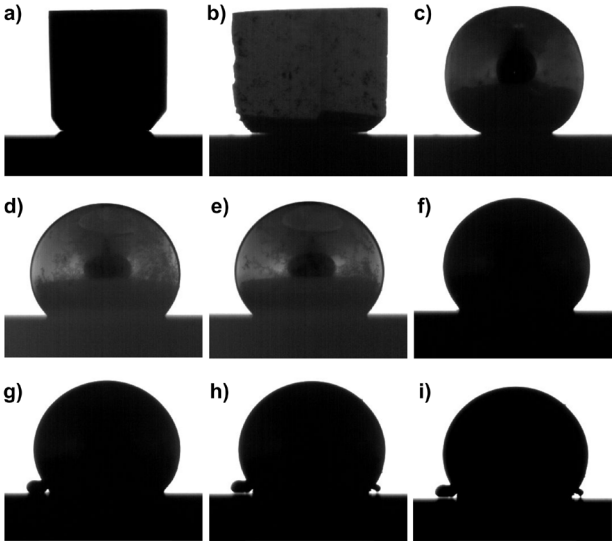

Fig. 3. Images of VG iron on Al_2O_3 substrate registered during high-temperature measurements: a) the beginning of heating, T = 21°C, b) the beginning of melting of cast iron sample, T = 1182°C, c) the formation of the drop, T = 1191°C, d) the start of the test at T = 1450°C (t = 0), e) the end of the test, T = 1450°C (t = 15 min), f) the end of the wetting kinetics, T = 1122°C, g) T = 1119°C, small daughter drop visible on the left side of the mother drop, h) T = 1102°C, small daughter drop visible on the right side of the mother drop, i) T = 105°C, the end of the experiment

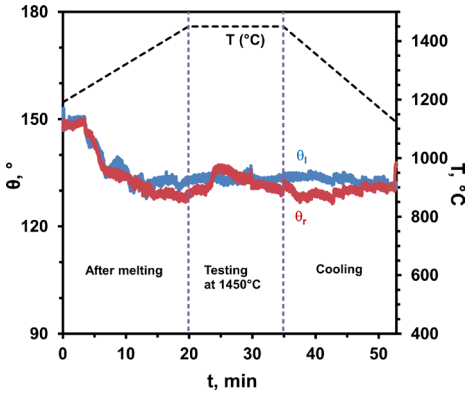

Fig. 4. Wettability kinetics of molten VG cast iron on Al_2O_3 substrate

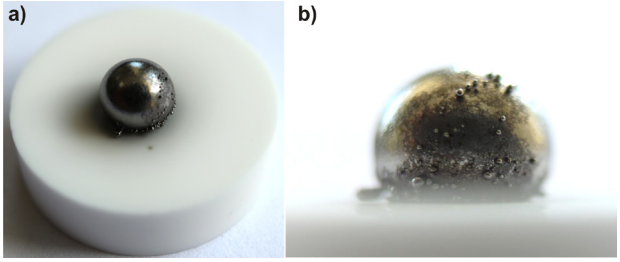

Fig. 5. Photo of solidified drop after high-temperature wetting test at T = 1450°C: top view (a), view of small droplets on the surface of main drop

A visual observation at the solidified drop of alloy after high-temperature investigation showed its spherical shape with a lot of small drops (daughter drops) visible on the surface main (mother) drop (Fig. 5) and created during the cooling of the cast iron/Al_2O_3 couple. The presence of these drops was probably associated with the outflow of melted, not yet solidified alloy from the interior of the main drop to the outside, as it was observed during wetting test shown in Figure 3. In the process of creation the satellite drops, the primary step was probably drop surface solidification, then the solidification of an inner (still liquid) phase, protruding through the surface layer due to the increase of the specific volume in the solid phase. This effect was registered as common phenomenon in cast irons [28]. Stefanescu et al. investigated the expansion of lamellar graphite iron (LG) and compacted graphite (CG) iron during its solidification using simultaneous thermal analysis (TA) and linear displacement analysis (LDA). Difference in expansion between LG and CG iron was small, but increases significantly with graphite nodularity. In relative numbers, when the solidification expansion of LG iron was 1, that of SG (spheroidal graphite) iron was 4.4, compared to 1 to 1.8 for CG iron [29]. In 2014 Alonso et al. studied the differences in the solidification mechanisms of irons with different graphite morphologies, namely: lamellar (flake), vermicular and spheroidal, at three different levels of carbon equivalent, to give hypoeutectic, eutectic and hypereutectic composition. Investigations found that graphite expansion increases with the carbon content and the magnesium residual. Spheroidal graphite iron had the highest expansion. Compacted graphite iron had slightly higher expansion than lamellar graphite iron [30].

Microstructure of VG cast iron in as-cast state was examined on the metallographic cross section using Zeiss Observer21.m optical microscope (OM) by using the magnifications up to 500×. The graphite morphology and distribution were identified based on PN-EN ISO 945-1 standard [31] while the structure of matrix – based on PN-75/H-04661 archival standard [32]. The materials in its as-cast state was characterized by ferritic-pearlitic structure (estimated fraction of ferrite was about 70−90%). The 98% of graphite precipitates had a vermicular morphology, while the rest of them was spheroidal.

The microstructure of cast iron sample (before and after wetting test) was also examined by SEM characterization combined with the local EDS analysis of the chemical composition of the sample (Table 2). Figures 6a−e present different sections of the same sample of VG cast iron in the as-cast state. Graphite precipitates had a vermicular morphology with an average length of about 45 μm while the rest precipitates were spheroidal with an average diameter of 50 μm.

SEM microstructures of cross-sectioned solidified sessile drop couple cast iron/Al_2O_3 and corresponding local EDS analysis in the marked points are presented on Figures 7a−j. The cross-section of the drop showed a structural homogeneity at low magnification (Fig. 7a). Observations under higher magnification (Figs. 7b−j) revealed graphite precipitates which took the shape of flakes having a different dispersion degree.

EDS results obtained on cast iron samples after high-temperature treatment are summarizes in Table 2. Points 1 to 7 in the table present the results of chemical composition of the VG cast iron before wettability test (Figs. 6a−e). Points 8−37 are the results registered in the cross-sectioned couple after wettability experiment.

SEM and EDS analysis showed that solidified cast iron/Al_2O_3 couple (Fig. 7c) has a layer about 26 μm thick on the drop-side interface between cast iron and Al_2O_3 substrate. It is composed mainly of carbon (82.08 at. %) and small amount of oxygen, iron and aluminum (point 16, Table 2). Similar chemical composition was recorded in the point 10 (Fig. 7b, Table 2). The results of EDS chemical composition analyses taken in points 26−37 on the top part of the drop did not reveal a presence of Al, that in turn was found in near drop-side interface area. Near the top of the drop (points: 27, 29, 32, 35, 36) the carbon and iron content suggest the formation of Fe_3C.

It should be highlighted that after solidification, the cast iron drop was found detached from the substrate. It made possible to perform the detailed structural characterization of the interfacial region and the results obtained were in a good agreement with findings from cross-section observations (Fig. 7c), i.e. high-temperature interaction between molten alumina substrate and cast iron of selected composition leads to the change of the structure and chemistry of not only the drop side interface but also the substrate side interfacial region, as it is schematically shown in Figure 8.

The above structural observations suggest that the drop side interfacial layer corresponds to the graphite phase nucleated at the alumina substrate during solidification while the substrate side region was formed due to the direct chemical reaction between alumina and the alloy. These findings are of practical importance since they put forward an idea to create composite materials with improved wear resistance by the introduction of ceramic reinforcement in cast iron matrix and promoting of graphite nucleation on the reinforcing particles [16].

More work and systematic studies are needed to clarify the mechanisms responsible for the formation of interfaces in molten cast iron/Al_2O_3 couple. Nevertheless, despite important discrepancies in literature data on factors affecting carbothermic reduction of alumina as well as occurrence and stability of possible reaction products (e.g. reported in [33−37]), it can not be excluded that under conditions of this study, the formation of aluminum oxycarbides can take place at the substrate side interface due to the following reactions between carbon (from the alloy) and alumina:

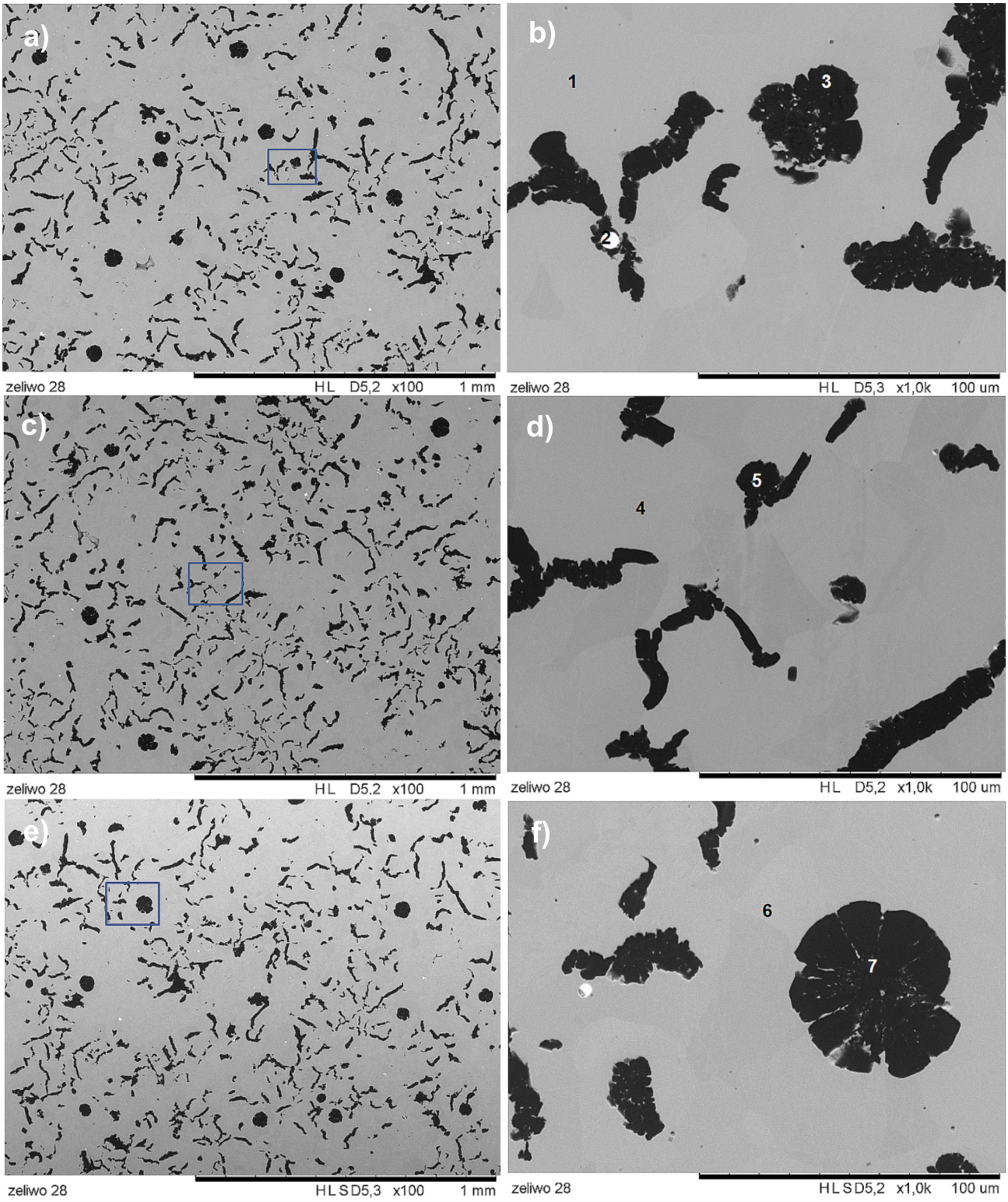

Fig. 6. SEM microstructures of vermicular graphite cast iron at as-cast state (a−e)

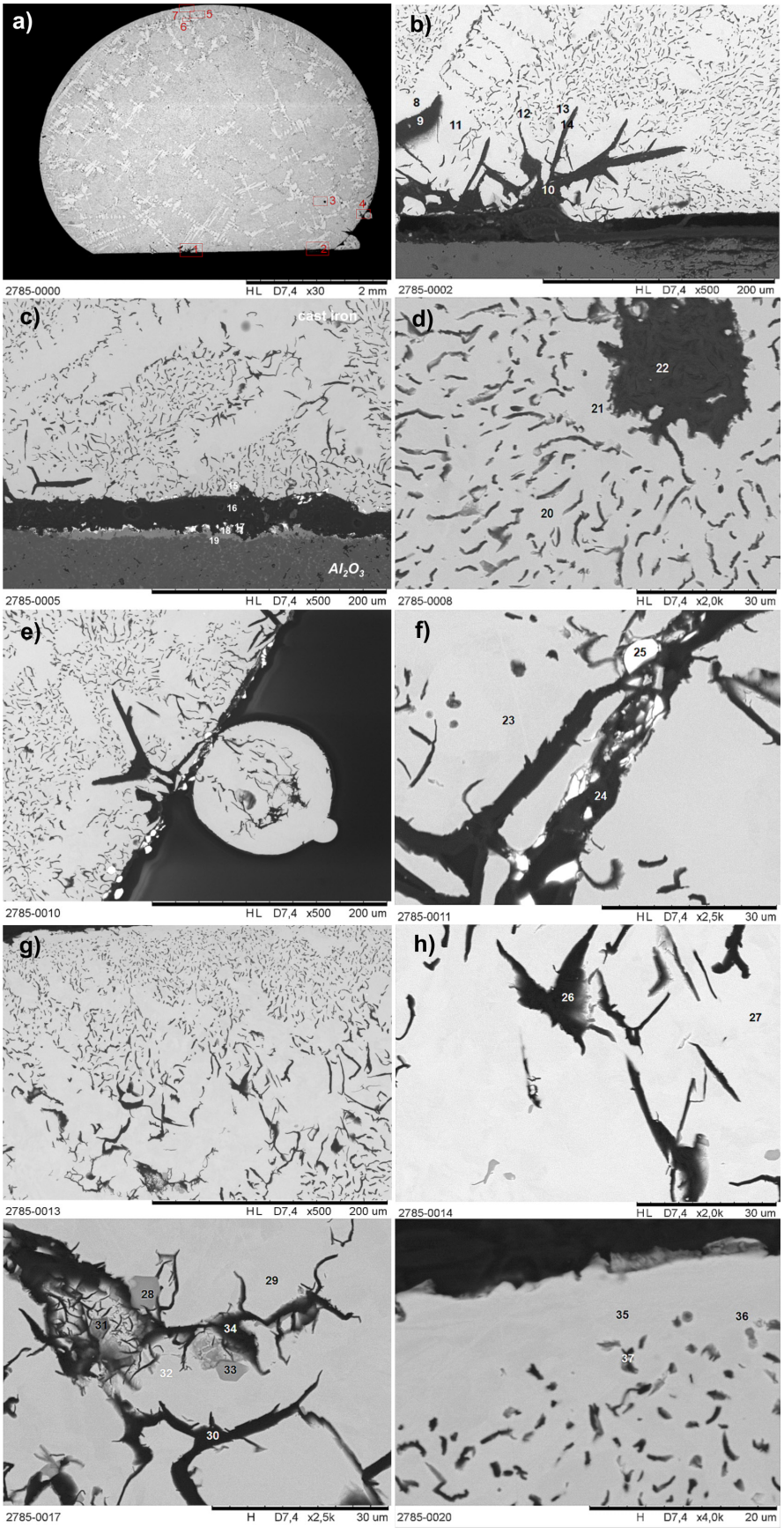

Fig. 7. SEM microstructures of cross-sectioned alloy/Al_2O_3 couple after wettability test: cross-section of solidified alloy drop with labelled areas from EDS measurements (a), area 1 (b), area 2 (c), area 3 (d,) area 4 (e−f), area 5 (g−h), area 6 (l), area 7 (j)

Table 2. Results of the local EDS analysis of chemical composition (at. %) made in cross-section of cast iron sample before and after wettability test at T = 1450°C (the points of EDS analysis are marked by numbers in Fig. 6 and Fig. 7, respectively)

Point	Fe	C	Si	Mg	P	Mn	S	O	Al
1	61.93	34.19	3.41	0.42	0.05	–	–	–	–
2	4.99	89.55	–	–	–	–	5.46	–	–
3	3.69	94.89	0.14	0.04	–	–	0.02	1.23	–
4	58.91	37.55	3.53	0.01	–	–	–	–	–
5	3.71	95.61	0.08	–	–	–	–	0.60	–
6	58.84	37.45	3.71	–	–	–	–	–	–
7	3.01	96.34	0.15	0.02	–	–	0.03	0.46	–
8	51.43	38.11	3.26	0.25	0.08	–	–	3.29	3.58
9	3.22	91.76	0.15	–	–	–	–	4.25	0.61
10	0.47	75.07	1.59	–	–	–	0.07	21.97	0.82
11	53.14	37.66	2.73	0.11	–	–	–	2.84	3.52
12	54.83	34.81	3.46	0.45	0.08	–	0.02	2.08	4.28
13	56.71	34.93	2.67	–	–	–	–	3.04	2.64
14	4.58	89.66	0.19	–	–	–	–	4.80	0.77
15	46.43	40.66	2.72	0.09	–	–	–	4.95	5.16
16	1.71	82.08	0.15	0.10	0.01	–	0.04	14.39	1.52
17	1.50	48.94	0.17	0.29	0.09	0.04	1.98	38.11	8.89
18	1.40	24.29	0.27	1.34	0.05	–	0.01	50.49	22.15
19	1.88	22.67	0.45	0.21	–	–	–	48.99	25.80
20	64.86	30.12	3.78	0.78	–	–	–	–	0.47
21	58.96	35.63	3.22	–	–	–	–	1.41	0.77
22	4.24	91.81	0.15	0.03	–	–	–	3.70	0.06
23	45.88	50.59	2.87	–	–	–	–	–	0.66
24	4.28	82.09	0.01	–	–	–	0.16	13.41	0.06
25	3.82	77.72	–	–	–	0.03	10.47	7.95	–
26	3.61	95.06	0.13	–	0.02	–	–	1.18	–
27	68.94	27.33	3.45	0.15	–	–	–	–	0.12
28	3.80	87.74	0.69	–	3.89	–	0.66	3.14	0.07
29	72.72	24.98	2.08	0.11	0.08	–	–	–	0.03
30	2.84	95.32	–	–	0.18	–	–	1.59	0.05
31	12.08	87.01	0.27	–	0.21	–	–	0.42	–
32	68.24	29.52	1.89	0.03	0.27	–	–	0.05	–
33	3.87	83.95	0.59	–	–	–	–	1.20	–
33	3.87	83.95	0.59	0.78	4.31	0.06	0.94	4.81	0.69
34	2.21	95.36	0.07	–	–	0.02	–	2.34	–
35	68.41	28.16	3.16	–	0.27	–	–	–	–
36	66.99	29.91	3.10	–	–	–	–	–	–
37	34.03	63.52	1.25	–	–	–	–	1.20	–
Measurement error: Fe – 2.19%; C – 2.33%; Si – 0.09%; Mg – 0.00%; P – 0.00%; Mn – 0.00%; S – 0.03%; O – 0.20%; Al – 0.00%									

$$Al_2O_3 + 3C = Al_2OC + 2CO(g) \quad (1)$$

$$2Al_2O_3 + 3C = Al_4O_4C + 2CO(g) \quad (2)$$

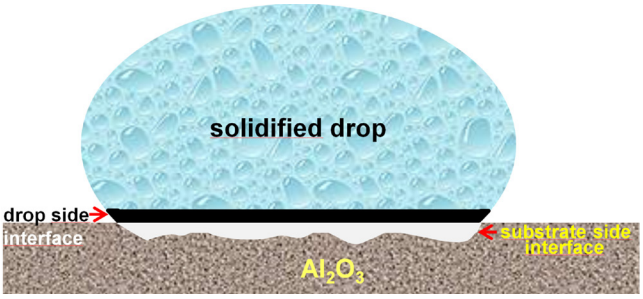

Fig. 8. Scheme illustrating the interaction zone of solidified drop of cast iron with Al_2O_3 substrate

Experimental results of EDS analysis of the interface (e.g. points 18 and 19 in Fig. 7c and Table 2) indicate that the substrate side interfacial layer is reach in both oxygen (about 50 at. %) and carbon (23−24 at. %). Taking into account that oxygen content in this layer is comparable to total amount of Al + C, it seems that chemical composition of reactively formed interfacial phase corresponds rather to the Al_4O_4C phase. This statement is in a reasonable agreement with recent findings regarding thermodynamic data relevant to the thermical process in Al-C-O system. Both thermodynamic calculations (e.g. [34−37]) as well as experimental data (e.g. [37]) show that Al_4O_4C oxycarbide is a more stable compound than Al_2O_3 and itself more stable than Al_2OC, which can occur when operating at much higher temperatures that that used in this study.

From point of view of the role of the structure and chemistry of interfaces in final properties of composite material, a special attention should be paid to the conditions that ensure to get high integrity of reinforcing ceramic particles with a metal matrix. Since the detachment of the Al_2O_3 substrate from the cast iron drop after its solidification, noted after wettability test in this study, one may suggest a weak interface formed and thus questionable quality of composite material produced from the same materials as the sessile drop couple. However, it should be taken into consideration that this effect occurs due to the stresses generated at high temperature during solidification and cooling that are caused from CTE mismatch of contacting materials – the substrate and the solidifying drop. Therefore, we suggest that the detachment of the cast iron drop from alumina substrate after the sessile drop test does not refer to operation conditions of a composite material that has to withstand erosion wear, i.e. the material produced from cast iron matrix and reinforced with ceramic particles. Furthermore, it is believed that the expansion of metal matrix volume, as common phenomenon in cast irons during solidification, makes the interfaces in the composite material more tight and durable thus ensuring high integrity of the reinforcing particles with the matrix.

4. Conclusions

1. Vermicular graphite cast iron after melting and holding at T = 1450°C for 15 min does not wet Al_2O_3 substrate and forms a high contact angle of 131°. Structural characterization of the interface formed between the drop of cast iron and alumina substrate in the wettability test revealed the formation of two interfacial layers. The drop side layer of about 26 μm thickness is mainly composed of carbon and it presents the graphite phase nucleated at the alumina substrate during solidification of the sessile drop couple. The substrate side interfacial layer was formed due to the direct chemical reaction between alumina and the alloy. The presence of aluminum oxycarbide Al_4O_4C in this layer is possible.

2. SEM microstructure combined with local EDS analysis for the sample of vermicular cast iron in as-cast state differs significantly from the microstructure of solidified VG cast iron drop. The regular structure of cast iron with vermicular graphite has changed and created structural heterogeneity in cross section after melting. Near the top of the drop the carbon and iron content suggest the formation of Fe_3C.

3. During the cooling of the cast iron/Al_2O_3 couple a lot of small satellite droplets were created on the surface of the main (mother) drop. The primary step of this process was probably drop surface solidification, followed by the solidification of an inner, still liquid phase, protruding through the surface layer due to increase of the specific volume during solidification of cast iron melt.

4. The results of this study are of practical importance since they put forward an idea to create composite materials with improved wear resistance by the introduction of ceramic reinforcement in cast iron matrix and promoting of graphite nucleation on the reinforcing particles.

Acknowledgements

The research were carried out with thanks to the financial support of the National Science Centre of Poland, project No. 2015/17/B/ST8/03391 entitled “High temperature investigations of the effect of alloying additions on thermophysical properties of liquid cast iron and its wettability and reactivity in contact with metal oxides”.

We would like to thank our Reviewers for their valuable comments and suggestions.

References

1. Laneri K.F., J. Desimoni, R.C. Mercader, R.W. Gregorutti, J.L. Sarutti. 2001. "Thermal dependence of austmpering transformation kinetics of compacted graphite cast iron". *Metallurgical and Materials Transactions A* 32 (1) : 51−58.

2. Kim S., S.L. Cockcroft, A.M. Omran, H. Hwang. 2009. "Mechanical, wear and heat exposure properties of compacted graphite cast iron at elevated temperatures". *Journal of Alloys Compounds* 487 (1−2) : 253−257.

3. Cueva G., A. Sinatora, W.L. Guesser, A.P. Tschiptschin. 2003. "Wear resistance of cast irons used in brake disc rotors". *Wear* 255 (7−12) : 1256−1260.

4. Dawson S., F. Hang. 2010. Compacted graphite iron – a material solution for modern diesel engine cylinder blocks and heads. In *Proceedings of 69th World Foundry Congress, Hangzhou, China, 2010, 16−20 Oct.*, 359−364.

5. Pytel A., E. Guzik. 2016. "Cast iron with vermicular graphite as a prospective material". *Transactions of Foundry Research Institute* 56 (4) : 301−319.

6. Masuda M., T. Sato, T. Kori, Y. Chujo. 1994. "Cutting performance and wear mechanism of alumina-based ceramic tools when machining austempered ductile iron". *Wear* 174 (1−2) : 147−153.

7. Heck M., H.M. Ortner, S. Flege, U. Reuter, W. Ensinger. 2008. "Analytical investigations concerning the wear behaviour of cutting tools used for machining of compacted graphite iron and grey cast iron". *International Journal of Refractory Metals and Hard Materials* 26 (3) : 197−206.

8. Guzik E. 2001. *Some selected problems concerning processes of cast iron improvement*. Katowice: Polish Academy of Sciences, Archives of Foundry Engineering, Monograph 1M.

9. Guzik E., S. Dzik. 2009. "Structure and mechanical properties of vermicular cast iron in cylinder head casting". *Archives of Foundry Engineering* 9 (1) : 175−180.

10. Guzik E. 2010. "Structure and mechanical properties as well as application of high quality vermicular cast iron". *Archives of Foundry Engineering* 10 (3) : 95−100.

11. Guzik E., D. Kopyciński, T. Kleingartner, M. Sokolnicki. 2012. "The structure and mechanical properties of pearlitic-ferritic vermicular cast iron". *Archives of Foundry Engineering* 12 (1) : 33−36.

12. Minkoff I. 1983. Solidification of spheroidal graphite cast iron (Chap. 5). In *The physical metallurgy of cast iron*, 102−133. Norwich: John Wiley&Sons.

13. Roviglione A., J.D. Hermida. 2004. "From flake to nodular: A new theory of morphological modification in grey cast iron". *Metallurgical and Materials Transactions B* 35B (2) : 313−330.

14. Riposan I., M. Chisamera, L. Sofroni, V. Brabie. 1985. Contributions to the study of the solidification mechanism ad of the influence of structure on the properties of compacted/vermicular graphite cast iron. In *The physical metallurgy of cast iron*, 131−140. Elsevier Science Publishing Co. Inc.

15. Gregorutti R.W., J.E. Grau. 2014. "Mechanical properties of compacted graphite cast iron with different microstructures". *International Journal of Cast Metals Research* 27 (5) : 275−281.

16. Hathaway R.M., P.K. Rohatgi, N. Sobczak, J. Sobczak. 1998. *Ferrous composites: A review.* In *Proceedings of 2nd International Conference "High Temperature Capillarity", 29 June−2 July 1997, Cracow, Poland*, eds. N. Eustathopoulos, N. Sobczak, 267−276. Kraków: Foundry Research Institute.

17. Kan W.H., C. Albino, D. Dias-da-Costa, K. Dolman, T. Lucey, X. Tang, L. Chang, G. Proust, J. Cairney. 2018. "Microstructure characterisation and mechanical properties of a functionally-graded NbC/high chromium white cast iron composite". *Materials Characterization* 136 : 196−205.

18. Dulska A., A. Studnicki, J. Szajnar. 2017. "Reinforcing cast iron with composite insert". *Archives of Metallurgy and Metals* 62 (1) : 355−357.

19. Podrzucki C. 1991. *Żeliwo, struktura, właściwości, zastosowanie. Tom 1*, 42−45. Warszawa: Wydawnictwo ZG STOP.

20. Pytel A., A. Gazda. 2014. "Evaluation of selected properties in austempered vermicular cast iron (AVCI)". *Transactions of Foundry Research Institute* 54 (4) : 23−29.

21. Sobczak N., M. Singh, R. Asthana. 2005. "High-temperature wettability measurements in metal/ceramic systems – Some methodological issues". *Current Opinion in Solid State Materials Science* 9 (4−5) : 241−253.

22. Sobczak N., M. Singh, R. Asthana. 2005. "High temperature capillarity and interfacial phenomena". *Current Opinion in Solid State Materials Science* 9 : 149−151.

23. Sobczak N., R. Nowak, W. Radziwill, J. Budzioch, A. Glenz. 2008. "Experimental complex for investigations of high temperature capillarity phenomena". *Materials Science Engineering A* 495 (1−2) : 43−49.

24. Sobczak N., J. Sobczak, R. Asthana, R. Purgert. 2010. "The mystery of molten metal". *China Foundry* 7 (4) : 425−437.

25. Eustathopoulos N., M.G. Nicolas, B. Drevet. 1999. *Wettability at High Temperatures*. Oxford: ELSEVIER SCIENCE Ltd. Pergamon Materials Series, ed. R.W. Cahn.

26. *ASTRA Reference Book*, IENI, Report, Oct., 2007.

27. Liggieri L., A. Passerone. 1989. "An automatic technique for measuring the surface tension of liquid metals". *High Temperature Technologies* 7 (2) : 82−86.

28. Tadesse A. 2017. *On the volume changes during the solidification of cast irons and peritectic steels*. Doctoral thesis. [Accessed 31 January 2018].

29. Stefanescu D.M., L. Dinescu, S. Craciun, M. Popescu. 1979. Production of vermicular graphite cast iron by operative control and correction of graphite shape. In *46th International Foundry Congress, CIATF Madrid, Spain, 1979*.

30. Alonso G., D.M. Stefanescu, R. Suárez, A. Loizaga, G. Zarrabeitia. 2014. "Understanding graphite expansion during the eutectic solidification of cast iron through combined Linear Displacement and Thermal Analysis". *International Foundry Research* 66 (4) : 2−12.

31. PN-EN ISO 945-1:2010. Mikrostruktura żeliwa. Cz. 1: Klasyfikacja grafitu za pomocą analizy wizualnej.

32. PN-75/H-04661. Żeliwo szare sferoidalne i ciągliwe. Badania metalograficzne. Określanie mikrostruktury (archiwalna).

33. Cox J.H., L.M. Pidgeon. 1963. "An investigation of the aluminum–oxygen–carbon system". *Canadian Journal Chemistry* 41 (3) : 671–683.

34. Halmann M., A. Steinfeld, M. Epstein, I. Vishnevetsky. 2014. "Vacuum carbothermic reduction of aluminia". *Mineral Processing and Extractive Metallurgy Review* 35 (2) : 126−135.

35. Sayad-Yaghoubi Y. 2011. "Selection of thermodynamic data for a novel carbothermic smelting process for aluminum". *JOM* 63 (5) : 30−34.

36. Lihrmann J.M. 2008. "Thermodynamics of the Al_2O_3–Al_4C_3 system: I. Thermochemical functions of Al oxide, carbide and oxycarbides between 298 and 2100 K". *Journal of the European Ceramic Society* 28 (3) : 633−642.

37. Yu Q., H. Yuan, F. Zhu, H. Zhang, C. Wang, D. Liu, B. Yang. 2012. "Carbothermic reduction of alumina with carbon in vacuum". *Journal of Central South University* 19 (7) : 1813−1816.